Grenze International Journal of Engineering and Technology, Jan Issue

CAD-Driven Approach with Enhanced Imaging and Deep Learning for Accurate Diagnosis of Brain Tumor

Jayashree Shedbalkar[1] and Dr. K. Prabhushetty[2]
[1]Department of Computer Science and Engineering, KLS VDIT, Haliyal, Visvesvaraya Technological University, Belagavi - 590018, KARNATAKA, INDIA.
E-mail: jayashri2512@gmail.com
ORCID id: https://orcid.org/0000-0002-9280-6516
[2]Research supervisor, Department of Electronics Communication and Engineering, SGBIT Belagavi, Visvesvaraya Technological University, Belagavi - 590018, KARNATAKA, INDIA.
E-mail: kprabhushetty1@gmail.com

Abstract— **Recently, the biomedical research field has become popular due to the use of digital image processing as the diagnosis of clinical patients has become more accurate and efficient with the help of Computer-Aided Diagnosis (CAD). Identifying diseases promptly and arranging treatment accordingly can improve the life quality and life expectancy of patients with brain tumors. Different tools have been designed to detect brain tumors, but the current diagnosis system utilizing Magnetic Resonance Imaging (MRI) scanning devices is expensive and often yields low accuracy and efficiency. To address this, a novel methodology utilizing CAD and different kinds of algorithms is proposed in this method to predict brain tumors more effectively. The proposed method uses a 2D Adaptive Bilateral Filter algorithm for image restoration to improve image quality. Additionally, it employs an Adaptive Histogram Adjustment algorithm to enhance brightness and contrast. For segmentation of the Region of Interest for brain tumors, uses the U-net algorithm and calculates various features with the convolutional neural network. With the aid of a Deep Convolutional Neural Network, it classifies disease images and stages using a Deep Learning approach. The proposed approach results in superior accuracy and efficiency in diagnostic decision-making compared to existing systems.**

Index Terms— CAD, MRI, AL (Artificial intelligence) 2D-ABF, AHA, U-Net segmentation, and deep learning neural network classifier.

I. INTRODUCTION

The field of Computer Aided Diagnosis (CAD) is an interesting area of research for Brain Tumor Disease (BT). In scientific research even though sharing of information is increasing, it is still uncertain whether a system designed based on one database will be suitable for other types of resources. Techniques such as conventional deep learning methods, even though they improve performance, are time-consuming and make it very difficult to collect evidence from various modalities. The proposed method uses systemic Magnetic Resonance Imaging (MRI). The goals of sMRI are to 1) enhance precision to match state-of-the-art methods, 2) find ways to overcome current challenges, and 3) investigate established brain indicators that aid in diagnosing BT.

MRI has proven to be an effective paradigm for brain analysis. Clinical images often need noise removal, which can be done using various techniques such as local measures, element investigation, and non-local measures like

Grenze ID: 01.GIJET.10.1.312

TANLM filters. A histogram of the structural association of images can be used to study the distribution of pixel brightness. To enhance the contrast of images, Histogram Equalization (HE) is used. Other popular methods such as Contrast Limited Adaptive Histogram Equalization (CLAHE) can also be used.
The dynamic model reflects the pixel similarity functions to optimize and control the intensity of each entity evolutionarily. [7]. MRI differentiation is implemented in a region of interest. The concept is to treat this issue as a classification task in which the goal is to differentiate between normal and abnormal elements on an MRI image based on several characteristics, including levels of intensity and shape.
The neural network is also suitable for different image classifications. The research explores how the CNN-related algorithm can be extended to a chest X-ray data set to identify pneumonia. The result from the experiments indicates that information increase is usually an efficient way to boost efficiency for all three algorithms. The second important factor is the difficulty of a system that fits the set of data measures [9]. The statistical method of several neurological diseases varies depending on the computerized and precise differentiation and structural categorization. The DL-based recognition and segmentation system have obtained research interest nowadays. The function extraction in the curvelet domain and CNN offer an improvement in precision compared with the wavelet transformation and identification utilizing conventional classification techniques such as SVM and Probabilistic Neural Network (PNN) [10].
In this research paper, section 2 consists of related works of various researchers, and the motivation behind this work is given. The proposed system is elaborated in section 3 and the results of the experiment are shown in section 4. Finally, section 5 concludes the entire research with future work.

II. Review Of Previous Studies

Krystyna Malik et. al [11] proposed a refined filter design based on the bilateral denoising methodology. This filter considers the color and temporal range of pixel elements to obtain related resemblances. The weight vectors are components of the marginal contact element, like the traditional bilateral filter. The Vector Median Filter (VMF) method is the most used filtering model, which determines its performance using the vector organizing principle for a collection of pixels in the processing window.
Jun Wang, et. al [12] has discussed momentum and magnetic data sets for different component-based transforms that are used to describe related functionality. Issues of uncertainty faced by most of them. This puts the implementation of noise removal before the implementation of component-based transformation and increases the accuracy of the results.
V. Anoopl, et. al [13] has proposed a method in which impulse noise reduction and Rician noise with the help of a Bilateral Filter (BF). To get efficient filter specifications, EGOA is added to the original noisy image. The results of the suggested denoising method are compared with the genetic algorithm (GA) and other BFs that have been used previously concerning various image quality measuring parameters. In a pixel neighborhood, the spectral range is defined with the parameters of the field (spatial) filter while the weights of the filter set (intensity) are proportional to the isotopic range of the pixel.
Rinkal Patel et. al [14] have designed the BT neuro-imaging research, where different brain regions/voxels are studied independently. The deep learning methodology is named "Sparse Inverse Covariance Analysis" for learning functionality in the brain field, with limited computing expense and densely the correct degree. Through implementing sparse restriction, excessive/noisy structural constraints are abolished by placing the component factor at zero, participating in the factor pairs becoming conditionally autonomous [22]. [23].
Jun Zhang et. al [19] have proposed structural magnetic resonance imaging (MRI) effective method for tumor detection. Ramy A. Zeineldin et. al [20] have developed DeepSeg, as a structure for modular decoupling. It consists of two main parts linked, centered on a connection of encoding and decoding. Various CNN models such as residual neural network (ResNet), deep convolutional network (DenseNet), and NASNet were used based on modified U-Net design. Runhong Zhang et. al [21] have adopted NGI-ADP surface design for limit equilibrium research, based on which the impacts of soft clay anisotropy on the deformation of the diaphragm wall in approaches to the study is analyzed.

A. Motivation

Brain tumor disease is a medical illness that produces loss of memory and cognitive impairment by the killing of brain cells. A degenerative form of Alzheimer's, the condition begins slightly and is slowly becoming worse. Brain image is a significant field of scientific study, findings for the diagnosis of brain disorders. The hippocampus is an essential part of the brain. A human typical activity is based on the Hippocampus features. It takes several hours for a doctor to physically section the Hippocampus. In this research, an improved method is used to separate the hippocampus region, based on the watershed segmentation methodology. Using two methods, the brain images were translated into binary form. The first solution is the principles of block say, mask, and marking, and the second method is the concept of top hat, mask, and marking. However, some portions of the image are found to contain holes that disrupt the segmentation phase. The image hole-filling strategies are applied to solve this issue, and relevant components are grouped into linked modules.

B. Existing Methodology and its Disadvantages

The existing method is to continuously separate regular tissues and irregular tissues through images of the MRI samples. Such MR brain images are observed to be distorted with Strength in objects of homogeneity that induce excessive variance in strength and noise that impair the output of brain image processing. Due to this type of substance, one form of normal tissue in MRI is incorrectly classified as another standard tissue which contributes to diagnostic error. The approach involves preprocessing using 2D wrapping-based Curvelet transformation for eliminating noise with adjusted contextual fuzzy C means procedure implies taking into consideration the spatial details and fragments of natural structures as the surrounding pixels are strongly associated and often spontaneously construct up the original participation matrix. The cancer cells are often segmented by the method. The conventional method is not capable of finding brain tumors.

III. PROPOSED METHOD

The proposed system consists of four steps: pre-processing, segmentation, feature extraction, and disease classification. A diagram of the proposed method is shown in Fig. 1. During the training period, a classification model is chosen and the training MRI Brain image is used as input to the network. The extracted features, along with the class labels, are used to train a classifier. The research introduces a modern predictive approach that uses magnetic resonance (MR) to segment the entire brain into image sequences and measure its density to diagnose disease. The relevant MRI brain images have been collected from the Brain Neuro-imaging Initiative (BNI) website. T1-weighted MRI was considered at 1.5 T level as given in the specification. The proposed automated clustering approach is considered on the image numerical anatomy and our proposed methodology is named as "head prototype" to restrict the MRI brain pixel range.

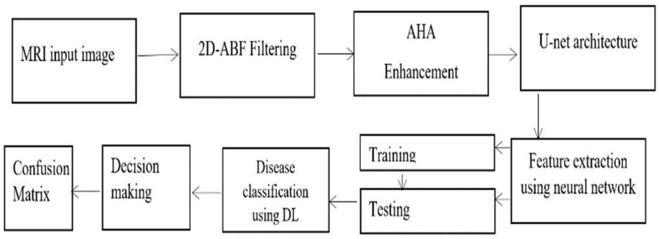

Figure1. Architecture diagram for the proposed methodology

A. MRI brain image pre-processing

The image restoration is completed using the 2D Adaptive Bilateral Filter (2D-ABF) algorithm. The 2D-ABF is used to eliminate unwanted noise like speckle noise, binary noise, and random noise. It is used to filter noises without degradation of original information content in MRI images. The 2D AHA is used to enhance visual contrast and brightness to enhance image consistency. The gray image is a useful format for MRI brain image segmentation. The MEM algorithm will cluster abnormal pixels on gray images.

B. Image Restoration using 2D Adaptive Bilateral Filter (2D-ABF)

De-noising has often been a research priority, yet there is still scope for progress, particularly regarding image de-noising. The biggest problem connected with this is the complexity of the calculation involved in making the convolution. The goal of image de-noising is to eliminate the noise whilst preserving as much clarity as possible of the essential image features such as boundaries.

The proposed image de-noising approach employs the 2D Adaptive Bilateral Filter. A difference between the original image and its de-noised version indicates the noise removed by the algorithm, which is considered as process noise. The system's vibrations act as a stimulus in theory. Although even high-quality images have some level of noise, it is reasonable to evaluate the effectiveness of various denoising techniques in this manner, without relying on the conventional approach of "adding noise and then removing it.". To be precise, it is known by.

$$MN = A - IF \quad (1)$$

A is the initial (not inherently noisy) image, and IF is the de-noising driver output for an input image A. This process interference in the Gaussian filter is negligible in harmonic sections of the image and very high close borders or texture, where the Laplacian cannot be low. To obtain what the bilateral filter takes out of the distorted image, the system noise concept is redefined as the gap between the distorted image and its opposed value. So, Eq. (1) is expressed as

$$MN = I - IF \quad (2)$$

Where I= A+Z is A distorted image acquired by destroying the initial image A by a white Gaussian distortion Z and IF is a Bilateral filter source for an input image I. The distortion of the system due to Gaussian filtering would have better borders relative to that of bilateral filtering because the borders are maintained by filtering spectrum (xr). Process noise MN is a mixture of image information D and a white Gaussian distortion N.

$$MN = D + N \quad (3)$$

Now the challenge is to approximate the information image D, which has just the actual image attributes and edges/sharp borders that the Bilateral filter eliminates, as reliably as necessary according to certain parameters and is merged with the Bilateral filtered image IF to get a stronger de-noise image with info. In class wavelet. Eq. (3) can be replicated as

$$Y = W + Nw \quad (4)$$

Where Y is a distorted wavelet coefficient (method noise). W is the real wavelet coefficient (detailed image) and Nw is Gaussian distortion-free.

C. Image Enhancement using 2D Adaptive Histogram Adjustment (2D-AHA)

2D Adaptive Histogram Adjustment (2D-AHA) image analysis used to boost or increase image intensity. AHA implements a method to correctly run the sub-image and merge it. The MRI image quality is improved by multiple histograms all relative to a single region of the image then utilized to reallocate image quality metrics like brightness or contrast calculation.

D. Proposed system

Step 1. Input (MRI image) is interpreted or perused.
Step 2. Change the MRI image into MRI at Gray Point.
Step 3. Add or conduct the Histogram Equalization technique to the image to maximize the image quality.
Step 4. Take the improved-image histogram.
Step 5. Consider or execute the Local Equalization Histogram (LHE). Apply method for improving image contrast on the input image (MRI image).
Step 6. Step 4 has to be repeated.
Step 7. Enable or execute Adaptive Histogram Adjustment (AHA). Apply the method for improving viewpoint intensity on the reference image (MRI viewpoint).
Step 8. Do again step 4.
Step 9. To improve image quality, apply or execute the quality-dependent adaptive histogram equalization technique on the input image.
Step 10. Repeat step 4

E .U-net segmentation

To improve the representation capacity of the segmentation network and to optimize the segmentation performance, we modify the U-Net architecture with an inspection module, which has been experimentally proven to enhance the capturing of more visual information under constrained computational complexity. As in Fig. 2. The inception module is redesigned where a 7x7 convolution layer enlarges the receptive field and the max pooling layer is replaced by a short path to directly incorporate the input filters. The output filter generated from the 1x1, 3x3, and 7x7 convolutional layers are concatenated with the input feature map to achieve feature fusion. To speed up the convergence and overcome the disadvantages of deep neural networks that are difficult to train. We adopt BN (batch normalization) to normalize the feature maps. shown in Fig.2.
Algorithm 1: The U-net segmentation process of the proposed model.
Input:

These image batches Z1 $=\left\{Z_1^{(1)}, Z_1^{(2)}, Z_1^{(3)}, \dots\dots\dots\dots, Z_1^{(M)}\right\}$, Z2= $\left\{Z_2^{(1)}, Z_2^{(2)}, Z_2^{(3)}, \dots\dots\dots\dots, Z_2^{(M)}\right\}$ and Z3=$\left\{Z_3^{(1)}, Z_3^{(2)}, Z_3^{(3)}, \dots\dots\dots\dots, Z_3^{(M)}\right\}$, initialized parameters of dual DCNNs and synergic network,$\theta^{(1)}$, $\theta^{(2)}, \theta^{(3)}$ and $\theta^{(s)}$, learning rate ɳ(t) and the hyper parameter λ.

Step 1: forward propagation:

Q1=q(Z1,θ(1))

Q2=q(Z2,θ(2))

Q3=q(Z3,θ(3))

Step 2: concatenate Q1,Q2 and Q3 to Q102 $=\left\{Q_{102}^{(1)}, Q_{102}^{(2)}, Q_{102}^{(3)}, \dots\dots\dots\dots, Q_{102}^{(M)}\right\}$ where $Q_{102}^{(1)}$ represents the combination of $Q_1^{(1)}$, $Q_2^{(1)}$ and $Q_3^{(1)}$. And input them to the synergic network. The labels of these four supervisions are

W1 $=\left\{W_1^{(1)}, W_1^{(2)}, W_1^{(3)}, \dots\dots\dots\dots, W_1^{(M)}\right\}$,

W2= $\left\{W_2^{(1)}, W_2^{(2)}, W_2^{(3)}, \dots\dots\dots\dots, W_2^{(M)}\right\}$

W3=$\left\{W_3^{(1)}, W_3^{(2)}, W_3^{(3)}, \dots\dots\dots\dots, W_3^{(M)}\right\}$, and

WS=$\left\{W_S^{(1)}, W_S^{(2)}, W_S^{(3)}, \dots\dots\dots\dots, W_S^{(M)}\right\}$,

Where,

$W_S^{(1)}$-1 if $W_1^{(1)} - W_2^{(1)}$, otherwise $W_S^{(1)} = 0$.

Step 3: update parameter $\theta^{(1)}, \theta^{(2)}, \theta^{(3)}$ and $\theta^{(5)}$ by using back-propagation algorithm .Compute loss:

$$p^{(1)}\,\theta^{(1)}, p^{(2)}\,\theta^{(2)}, p^{(3)}\,\theta^{(3)}\ and\ p^{(s)}\,\theta^{(s)}. \qquad (5)$$

Compute gradient:

$$\Delta^{s} = \frac{\partial p^{s}(\theta^{(s)})}{\partial \theta^{s}} \qquad (6)$$

$$\Delta^{(1)} = \frac{\partial p^{(1)}(\theta^{(1)})}{\partial \theta^{(1)}} + \lambda \Delta^{s} \qquad (7)$$

$$\Delta^{(2)} = \frac{\partial p^{(2)}(\theta^{(2)})}{\partial \theta^{(2)}} + \lambda \Delta^{s} \qquad (8)$$

And

$$\Delta^{(3)} = \frac{\partial p^{(3)}(\theta^{(3)})}{\partial \theta^{(3)}} + \lambda \Delta^{s} \qquad (9)$$

Update parameters:

$$\theta^{(1)}(t+1) \leftarrow \theta^{(1)}(t) - ɳ^{(t)}.\Delta^{(1)}$$

$$\theta^{(2)}(t+1) \leftarrow \theta^{(2)}(t) - ɳ^{(t)}.\Delta^{(2)}$$

$$\theta^{(3)}(t+1) \leftarrow \theta^{(3)}(t) - ɳ^{(t)}.\Delta^{(3)}$$

And

$$\theta^{(s)}(t+1) \leftarrow \theta^{(s)}(t) - ɳ^{(t)}.\Delta^{(s)} \qquad (10)$$

When applying the trained SDLR model to the classification of a test image x, each DCNN component DCNN. j gives a prediction vector R(1)= $R_1^{(1)}, R_2^{(1)}, R_3^{(1)}, \dots\dots\dots\dots, R_K^{(1)}$, which is the activations in its last fully connected layer. The class label of this test image can be predicted as

$$W(x) = arg_j max\left\{\sum_{i=1}^{n} R_1^{(1)} \dots . \sum_{i=1}^{n} R_j^{(1)} \dots . . \sum_{i=1}^{n} R_k^{(1)}\right\} \qquad (11)$$

F. Global and Local Features Extraction

We investigate the two major portraying the substance of a picture, we remove worldwide element and neighborhood highlights with Faster DCNN. We separate worldwide component from fe7 layer of VGG16 net, a 4096-measurement vector indicated as Gf. We select top n recognized articles to speak to significant nearby items as indicated by their group certainty scores acquired from DCNN. Each picture can be at long last spoken to as a lot of 4096-measurement vectors1= {Gf,Lf1…….Lfn }. In our tests, we set n to 10 since the quantity of item contained in a picture is as a rule beneath 10.

G. Global-local information Mechanism

The local information with global information is major model for describing frame. In our proposed model, we assume recognition mechanism to synthesize those two models of information according to the subsequent Eq.

$$\Psi^{(r)}(i) = \alpha_D^{(r)} Gf + \sum_{i=1}^{n} \alpha_i^{(l)} Lf_1 \qquad (12)$$

Where $\alpha_i^{(l)}$represent the information load of separate attribute at time t and $\sum_{-t} \alpha^{(t)} = 1$.

This component progressively loads each element by allocating it with one positive weight $\alpha_l^{(t)}$alongside the sentence age method. The consideration weight $\alpha_l^{(t)}$ measures significance level of each component at time t and the pertinence of each element to the past data. Subsequently, it very well may be registered dependent on the past data and each element $f_1 \in \{Gf, Lf_0, \dots \dots \dots \dots . . Lf_n\}$ with the accompanying conditions:

$$\beta_1^{(r)} = \omega^t \varphi\left(W_h h^{(t-1)} + W_h f_t + b\right),$$

$$\alpha_l^{(t)} = \frac{\beta_t^{(r)}}{\sum_{j=0}^{n} \beta_1^{(t)}} \qquad (13)$$

where $\beta_t^{(r)}$represent as score of attributes and previous creating text as fi

The information heavy load is obtained by standardize SoftMax reversion H(t-1) is the past concealed state yield which will be presented in the following segment W, Wh , W, and b are the parameters to be learned by our model and shared by every one of the highlights at all the time steps ϕ is initiation work.

H. Deep Convolutional Neural Network

Deep Convolutional Neural Network (DCNNS) is CNNS with numerous layers and mirror the guideline of order. After a few convolutional layers, profound CNNS commonly include one or a couple completely associated layers, that is, layers where the weight framework W is thick. The explanations behind doing as such are to some degree blended and not so convincing. The yield from a profound CNN is encouraged to a calculation that relies upon the motivation behind the net. For regression, for instance, the outputs may be used as they are. For classification, one could use the outputs as inputs to a support vector machine or random forest or, if the classifier requires input quantities that behave like probabilities, the output stage could be a soft max function.

$$z\, \sigma(y) = \frac{\exp(y)}{1^7 \exp(y)} \qquad (14)$$

Where l is section vector of ones. Logically, the exponential makes all amounts positive, and standardization ensures the passages of Z signify 1. The motivation behind why this capacity is classified “softmax” is that on the off chance that one of the yi sections state y0, is a lot greater than the majority of the others, at that point lr exp(y)= exp(yrϕ) ,so that

$$z_{i0} \approx 1 \; and \; z_j \approx 0 \; for \; i \neq i_0,$$

And the function effectively acts as an indicator of the largest entry in y. Somewhat more precisely, and quite obviously,

$$\lim_{\alpha \to x} y^r \sigma(\alpha y) = mx(y) \qquad (15)$$

In summary, a deep CNN performs the following computation:

$$x(0) = x \qquad (16)$$

$$x(l) = \pi\left(h\left(W^{(1)} \underset{x}{\leftarrow}^{(l-1)}\right)\right) \; for \; l = 1, \dots \dots \dots \dots \dots l_\propto \qquad (17)$$

$$x(l) = \left(h\left(W^{(1)} \underset{x}{\leftarrow}^{(l-1)}\right)\right) \; for \; l = L_\propto + 1 \dots \dots \dots \dots \dots L \qquad (18)$$

$$y = h_f\left(x^{(l)}\right) \qquad (19)$$

Where the yield initiation work hy might be the character, SoftMax, or other capacity. The networks W(I) have D(l-1) + 1 segments with D (0) – D and D (1) for 1>0 being equivalent to the quantity of yields (or enactments) in layer number 1. The first Le layers are convolutional, and the staying ones are completely associated.

The convolutional layers fill in as highlight extractors, and in this way, they become familiar with the element portrayals of their information pictures. Inputs are convolved with the informed loads to figure another segment map, and the convolved results are sent through a nonlinear establishment work. All neurons inside a component map have loads that are obliged to be equal; be that as it may, distinctive component maps inside the equivalent

convolutional layer have diverse loads so a few highlights can be extricated at every area the kth yield include map Yt.
The deep study shows a frame recognition, got from convolutional layer. This leads a major role to DCNN with various kind of filters to represent a complete frame. It maps an intermediate attribute and creates different region maps (Fig.3). It will do mapping from given input attribute to hidden layers. The input layer will pass the frame to the hidden layer. And it has 3 various hyper functions to control the length of the output layer in convolution. We also described zero padding, depth, and stride. For example, convolution took the input frame as input, and we mentioned various neurons in depth size may initialize here.

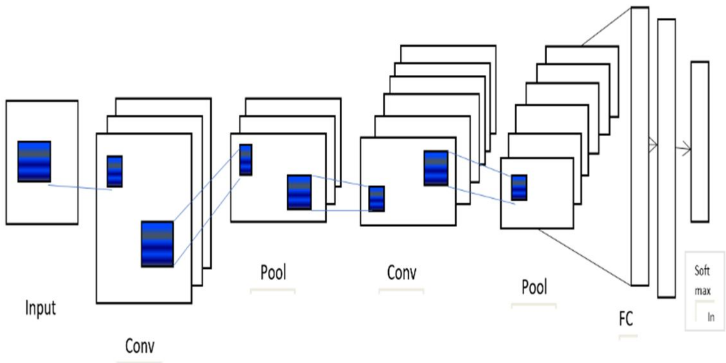

Figure 3. The Deep convolutional neural network using various layer.

$$Yi = f(Wk*x) \quad (20)$$

byx is indicated as input frame: WK is indicated with kth attribute, which is like convolutional filter. It is used to evaluate the pixel ratio of every single frame and f(.) denotes the nonlinear trigger task. Their image and attainment have given to a zone of exploration that points out the advancement and use of DCNN actuation capacities to improve a few qualities of DCNN execution.

H. Pooling Layers

These are occasionally embedded after each convolutional layer to diminish the dimensionality of the system. Its errand involves unraveling or lessening the spatial components of the information got from a part map. There are 3 sorts of pooling:
Firstly, we used the normal method for pooling, then L2-standard is used in second term for pooling outstanding usage in its speed and improved association. This essentially takes a channel and a walk of a similar length. It at that point applies it to the info volume and yields the greatest number in each sub district. That has the channel which convolves around.

$$Y_{kg} = \max_{lpq\alpha N_q} \; x_{kyq} \quad (21)$$

I. FC layers

Some pooling and convolutional layers are commonly stacked over one another to extricate increasingly unique element portrayals in traveling over the network. This layer follows information related performance in high level tasks. Every one of the sources of info is associated with all the yields thus the expression "completely associated". It is the last layer, as a rule after the last pooling layer in CNN process (Figure 1). Completely associated layers perform like a conventional neural system and contain about 90% of the parameters in CNN. This layer essentially takes info the yield of the last pooling layer and yields a N dimensional vector where N is the quantity of classes that the program needs to browse. For picture grouping, we could nourish forward the vector into certain number classes. The yield is additionally a vector of numbers.

J. LSTM

The separate input creation image can hide a vector output in LSTM. Fig.3 shows the results as every single cell (e) It accepts LSTM layer arranged by ht-1 and x, as given input. This scalar product with four various gates in weights (w). Every gate has a various function one.
LSTM equation represent as,

$$\begin{pmatrix} i \\ f \\ o \\ g \end{pmatrix} = \begin{pmatrix} \sigma \\ \sigma \\ \sigma \\ tanh \end{pmatrix} W \begin{pmatrix} h_{(0-1)} \\ x_t \end{pmatrix} \quad (22)$$

$$c_{t=}f * c_{i-l} + i * g \quad (23)$$

$$h_t = o * \tanh(c_t) \quad (24)$$

The CNN was represented by LSTM, this layer acknowledges the contributions and secondly, it gets successive yields of past model of LSTM. At last, we pertain a yield into complete associated surface and compute the last score SoftMax. Where o speaks to sigmoid capacity, and * is component insightful duplication. LSTM has a continuous inclination stream we develop our LSTM engineering for video grouping shown in Fig. 4.

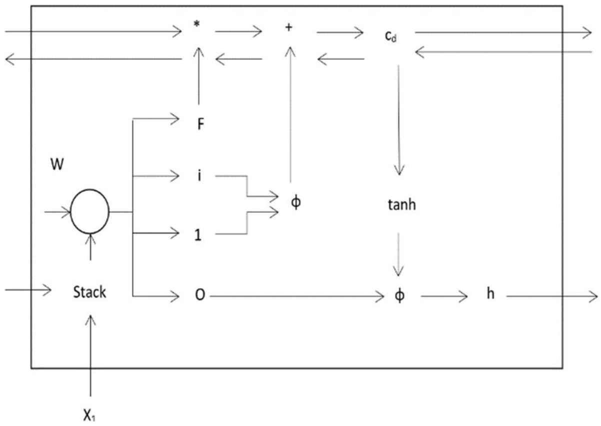

Figure 4. The four layers with LSTM cell

The four layers are:

1. Forgot gate layer: $ft = \sigma(u_f x_1 + w_f h_{\gamma-1} + b_f$
2. Input gate layer: $i_t = \sigma(m_i x_1 + w_1 ft_{\gamma-1} + b_i$
3. Candidate values computation layer: $\overrightarrow{c_t} = \tan h(u_t x_1 + w_t h_{t-1} + b_c)$
4. Output gate layer: $o_t = \sigma(u_\phi x_1 + w_\phi h_1 + b_x)$

The component insightful use of the sigmoid capacity (0), the overlook, information, and yield entryway layers (1. 2, and 4 above) produce vectors whose sections are altogether involved somewhere in the range of 0 and 1. and either near 0 or near 1. When one of these layers is duplicated with another vector, it in this manner goes about as a channel that just chooses a specific extent of that vector. The two outrageous cases are the point at which all sections are equivalent to 1 - the full vector passes-or to 0 - nothing passes. The parameters are anyway shared over unequaled advances.

K. Forgetting/learning:

By considering the new training example x, and the current hidden state he 1, the forget gate layer determines how much of the previous cell state c_{0-1} should be forgotten (what fraction of the memory should be freed up). While from the same input, the input gate layer decides how much of the candidate values č, should be given to the memory, or in various letters, how much of the new information should be learned. Combining the output of the two filters updates the cell state:

$$C_i = f_i * c_{i-1} + i,* \overline{c_\iota} \quad (25)$$

Where • denotes element wise multiplication. This way, important information is not overwritten by the new inputs but is able to be kept alongside them for long periods of time. Finally, the activation ht is computed from the updated memory, modulated by the output gate layer $o_{1:}$

$$H_l = \tanh c_l * o_l \quad (26)$$

The yield door enables the unit to possibly enact when the in-memory data is observed to be significant for the present time step. Finally, as before with the basic RNN, the yield vector is registered as a component of the new shrouded state.

$$Y_r = soft \max (Vh_r) \tag{27}$$

IV. Results

The experiments are done based on different standards of gray-scale MRI images with different sizes. The MRI images are corrupted by salt and pepper noise, speckle noise and random noise produced by MRI scanning devices as shown in Figure 5 (a). The 2D Adaptive Bilateral Filter (2D ABF) is applied to noise corrupted images to remove all noises without degradation of original content of image as shown in Figure 5 (b). To authorize the suggested methodology, their presentation is evaluated in terms of visual quality, PSNR and MSE are computed and tabulated using proposed algorithm called 2D ABF.

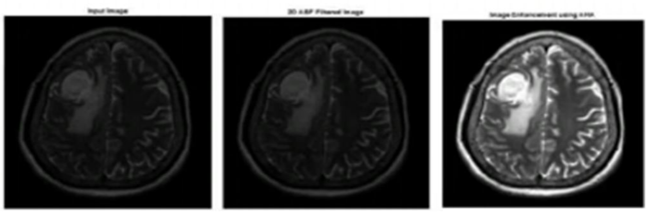

Fig.5. (a) Input MRI image, (b) 2D ABF Filtered Image, (c) Image Enhancement using AHA The figure 5 (c) shows enhancement image using Adaptive Histogram Adjustment (AHA) by improvement of contrast and brightness. The quality of image is improved using AHA algorithm.

Fig.6. (a) Image Clustering using UNet algorithm, (b) Tumor segmentation using UNet algorithm, (c) ROC Curve

The different intensity pixels are grouped using U-net segmentation algorithm. The Bayesian Threshold technique is applied to U-net segmentation algorithm to segment BT as displayed shown in Fig 6. (a)shows ROC curve of DCNN classifier. The 4.2 (c) shows Area Under Curve (AUC) value is 98 %.

TABLE II. IMAGE QUALITY MEASUREMENT

Metrics	Anisotropic Filter	Bilateral Filter	Proposed Method
PSNR	26.56	30.68	35.92
SSIM	0.7823	0.8453	0.9125
MSE	0.0044	0.0028	0.00052

TABLE II. IMAGE THE EFFECT OF VARYING THRESHOLD AND 'I' VALUES ON THE ACCURACY OF SOLITARY NODULES DETECTED. 'N' IS THE NUMBER OF SOLITARY NODULES DETECTED.

Dataset	*Threshold*	*i=10*		*i=10*	
		AGWO-ONN		AGWO-CNN	
		Accuracy	N	Accuracy	N
Publically available BIDC Dataset	0.65	97.0	44	97.6	44
	0.75	85	38	85	38
	0.85	66.67	20	66.7	20
In-house Clinical Dataset	0.65	90.7	34	92.5	34
	0.75	82	27	85.33	30
	0.85	60.76	21	62.15	24

On varying the threshold value there is an effect on the number of solitary nodules detected in widely available BIDC Dataset and In-house Clinical Dataset (Table 2). The threshold value is proportional to accuracy.

TABLE III. SEGMENTATION PERFORMANCE MEASURES OF DICE PARAMETER

Images	*Dice*			
	Otsu segmentation	Fuzzy C Means clustering	Watershed Segmentation	Proposed Method
Sample 1	0.0036	0.1472	0.0045	0.1520
Sample 2	0.0052	0.2295	0.0030	0.2459
Sample 3	0.0026	0.2086	0.0052	0.1965
Sample 4	0.0036	0.2426	0.0123	0.2993
Sample 5	0.0014	0.1611	0.0053	0.1526
Sample 6	0.0060	0.1639	0.0040	0.2337
Sample 7	0.0047	0.144	0.0045	0.174
Sample 8	0.0011	0.2114	0.0012	0.165
Sample 9	0.0015	0.1774	0.0034	0.147
Sample 10	0.0014	0.166	0.0012	0.159
Sample 11	0.0016	0.244	0.0032	0.1357
Sample 12	0.0011	0.144	0.0014	0.1258
Sample 13	0.0015	0.2354	0.0074	0.147
Sample14	0.0030	0.177	0.0094	0.1357
Sample 15	0.0064	0.166	0.0041	0.2147
Sample 16	0.0041	0.1254	0.0045	0.2413
Sample 17	0.0056	0.1337	0.0054	0.247
Sample 18	0.0021	0.1247	0.0041	0.195
Sample 19	0.0023	0.100	0.00624	0.1854
Sample 20	0.0041	0.2654	0.0081	0.17354
Average	0.0037	0.1922	0.0057	0.2133

TABLE IV. PERFORMANCE ANALYSIS OF THE RESNET-50

Classifier	Data (Testing- Training)	Type of Class	Sensitivity	Specificity	Precision	Accuracy
ResNet-50	90%-10%	Benign	0.959	0.961	0.919	0.722
		Malignant	0.915	0.896	0.942	
		Avg. Value	0.935	0.928	0.931	
	80%-20%	Benign	0.915	0.941	0.941	0.957
		Malignant	0.974	0.967	0.942	
		Avg. Value	0.945	0.954	0.94	
	70-30%	Benign	0.963	0.976	0.974	0.803
		Malignant	0.931	0.961	0.964	
		Avg. Value	0.947	0.969	0.969	
	85%-15%	Benign	0.941	0.957	0.931	0.849
		Malignant	0.942	0.917	0.9740	
		Avg. Value	0.9415	0.937	0.9525	
	70%-30%	Benign	0.950	0.935	0.9665	0.808
		Malignant	0.975	0.954	0.9388	
		Avg. Value	0.9625	0.9445	0.9525	

V. DISCUSSIONS

The Computer Aided Diagnosis (CAD) system is proposed using various algorithms to detect and classify brain tumor on MRI real images. The automatic segmentation and classification of BT in MRI brain images is implemented. The proper preprocessing is applied on the tool using 2D Adaptive Bilateral Filter (2D ABF) and

Adaptive Histogram Adjustment (AHA). The segmentation ROI is done using U-Net architecture system. The various image features are retrieved using neural network and the DCNN classification technique is used to classify normal and abnormal images. The accuracy of classification is more than 95.7% using DCNN.

FUTURE WORK

In future, CAD system may be applied for cancer cells identification by proper segmentation of Gray Matter (GM), White Matter (WM) and CSF. The adaptive clustering technique can be applied to segment disease region without pixels' error. DCNN can be applied to distinguish regular and anomalous MRI brain images.

REFERENCES

[1] Wei Li, Yifei Zhao, Xi Chen, Yang Xiao, Yuanyuan Qin, "Detecting Alzheimer's Disease on Small Dataset: A Knowledge Transfer Perspective", IEEE 2018,

[2] Samsuddin Ahmed, Kyu Yeong Choi, Jang Jae Lee, Bycong C. Kim, Goo-Rak Kwon , Kun Ho Lee and Ho Yub Jung, "Ensembles of Patch-Based Classifiers for Diagnosis of Alzheimer Discases", doi:10.1109/ACCESS.2019.2920011.

[3] Jun Zhang. Yue Gao,Yaozong Gao, Brent C. Munsell, Dinggang Shen, "Detecting Anatomical Landmarks for Fast Alzheimer's Disease Diagnosis", DOI 10.1109/TMI.2016.2582386, IEEE 2016.

[4] M. A. Balafar, "New spatial bused MRI image de-noising algorithm", DOI 10.1007/s10462- 011-9268-0.

[5] Fabrizio Russo, "Validation of Denoising Algorithms for Medical Imaging", Springer 2010.

[6] Saritha Saladi .N. Amutha Prabla, "Analysis of denoising filters on MRI brain images", DOI: 10.1002/ima 22225, btps://www.rescarchgate.net/publication/319163534.

[7] Chiao-Min Chen,Chih-Cheng Chen, Ming-Chi Wu, Gwoboa Horng, Hsien-Chu Wu, Shih- Hua Hsuch, His-Yun Ho, "Automatic Contrast Enhancement of Brain MR Images Using Hierarchical Corelation Histogram Analysis", DOI 10.1007/s40846-015-0096-6.

[8] Ramy A. Zeineldinl - Mohamed E. Karar2 - Jan Coburger3 - Christian R. Wirtz3 - Oliver Burgert 1, "DeepSeg deep neural network framework for automatic brain tumor segmentation using magnetic resonance FLAIR images", Springer 2020, International Journal of Computer Assisted Radiology and Surgery.

[9] MRI brain dataset, https://www.kaggk.com/navoneelbrain-mri-images-for-brain-tumor- sdetection.

[10] Estimation of Diaphragm Wall Deflections for Deep Braced Excavation in Anisotropic Clays Using Ensemble Learning. Geoscience Frontiers. DOI: 10.1016/jgsf.2020.03.003

[11] Wengang Zhang. Chongzhi Wu, Haiyi Zhong. Yongqin Li, Lin Wang, "Prediction of undrained shear strength using extreme gradient boosting and random forest based on Bayesian optimization" Geoscience Frontiers, 2020.

[12] Raouia Ayachi and Nahla Ben Amor, "Brain Tumor Segmentation Using Support Vector Machines", Springer 2009. (9),

[13] Samir S. Yadav and Shivajirao M. Jadhav, "Deep convolutional neural network based medical image classification for discase diagnosis", Springer 2019. (10).

[14] P. Muthu Krishnammal and S.Selvakumar Raja. "Convolutional Neural Network based Image Classification and Detection of Abnomalities in MRI Brain Images", IEEE 2019.

[15] Krystyna Malik and Bogdan Smolka, "Modified Bilateral Filter for the Restoration of Noisy Color Images", Springer 2012. (12].

[16] Jun Wang and Xinohong Meng. "Employing the bilateral filter to improve the derivative- based transforms for gravity and magnetie data sets", DOI: 10.1007/s11200-018-0162-y 4.

[17] V. Anoopl and P. R. Bipin, "Medical Image Enhancement by a Bilateral Filter Using Optimization Technique", Springer 2019.

[18] Rinkal Patel, Jun Liu, Kewei Chen, Erie Reiman, Gene Alexander and Jieping Ye, "Sparse Inverse Covariance Analysis of Human Brain for Alzheimer's Disease Study", IEEE 2019.

[19] Mostafa Amin-Naji, Hami Mahdavinataj and Ali Aghagolzadeh, "Alzheimer's disease diegnosis from structural MRI using Siamese convolutional neural network", IEEE 2019.

[20] Shunthi K J, Ravish DK and Dr. M Sasikumar, "Image segmentation an early detection to Alzheimer's disease", D01: 10.1109/INDCON.2013.6726006.

[21] R. Thillaikkarasil and S. Saravanan, "An Enhancement of Deep Learning Algorithm for Brain Tumor Segmentation Using Kernel Based CNN with M-SVM", Springer 2019.

[22] G. K. Reynokls: LM. Nir : N. Jahanshad :G. Prasad : P. M. Thompson, "Using the raw diffusion MRI signal and the von Mises-Fisher distribution for classification of Alzheimer's disease", 2014 IEEE 1lth International Symposium on Biomedical Imaging (ISB). DOI: 10.1 100/ISBL 2014.686848

[23] Jun Zhang, Member, IEEE, Mingxia Liu, Member, IEEE, Le An, Yaozong Gao, Dinggang Shen , Senior Member, IEEE, "Alzheimer's Disease Diagnosis using Landmark-based Features from Longitudinal Structural MR Images", 2168-2194 (e) 2016 IEEE.